Tempered fractional time series model for turbulence in geophysical flows

Mark M Meerschaert[1], Farzad Sabzikar[1], Mantha S Phanikumar[2] and Aklilu Zeleke[3]

[1] Department of Statistics & Probability, Michigan State University, East Lansing, MI 48824, USA
[2] Department of Civil and Environmental Engineering, Michigan State University, East Lansing, MI 48824, USA
[3] Lyman Briggs College and Department of Statistics and Probability, Michigan State University, East Lansing, MI 48824, USA

E-mail: mcubed@stt.msu.edu, sabzika2@stt.msu.edu, phani@msu.edu and zeleke@stt.msu.edu

Abstract. We propose a new time series model for velocity data in turbulent flows. The new model employs tempered fractional calculus to extend the classical 5/3 spectral model of Kolmogorov. Application to wind speed and water velocity in a large lake are presented, to demonstrate the practical utility of the model.

J. Stat. Mech. (2014) P09023

Contents

1. Introduction

Kolmogorov [1,2] proposed a model for the energy spectrum of turbulence in the inertial range, predicting that the spectrum $f(k)$ would follow a power law $f(k) \propto k^{-5/3}$ where k is the frequency. Kolmogorov based this prediction on a dimensional analysis, and confirmed it with experimental data [3]. Mandelbrot and Van Ness [4] pointed out the Kolmogorov spectrum corresponds to a stochastic process they termed fractional Brownian motion, defined as the fractional integral of a Brownian motion. The fractional Brownian motion with Hurst scaling index $H = 1/3$ exhibits the Kolmogorov spectrum, and hence provides a stochastic process model for turbulence in the inertial range.

Figure 1 illustrates the complete Kolmogorov spectral model for turbulence, and the power law approximation in the inertial range. Large eddies are produced in the low frequency range. In the inertial range, larger eddies are continuously broken down into smaller eddies, until they eventually dissipate, in the high frequency range. The inertial range prediction has been verified by a number of earlier studies based on data collected in the oceans [5], lakes [6] and the atmospheric boundary layer [7]. For more details, see for example [8,9].

In applications, one usually collects data on turbulence at regular time intervals. These time series can be modeled as a fractional Brownian motion sampled at discrete time points, or more directly as a time series. A time series model called ARFIMA, whose fractional difference is a Gaussian white noise sequence of uncorrelated random variables, is the discrete time analogue of a fractional Brownian motion. Hence it can serve as a useful discrete time stochastic model for turbulent velocity data, that captures the Kolmogorov scaling in the inertial frequency range.

In this paper, we describe and validate a new time series model for turbulence, called the ARTFIMA, that can fit turbulent velocity data over the entire frequency range. The ARTFIMA power spectrum behaves like a negative power law of frequency for moderate frequencies, but remains bounded as the frequency tends to zero. The new model is based on tempered fractional calculus, which is more flexible than the fractional calculus used
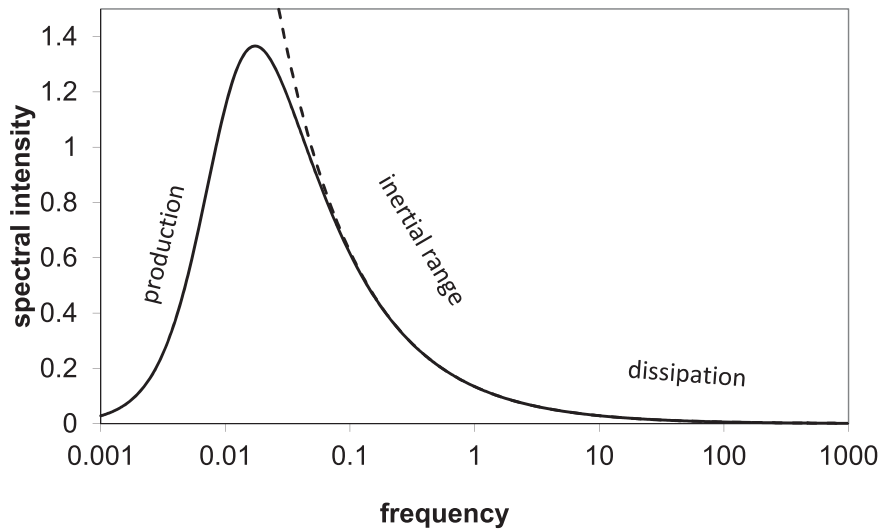
Figure 1. Kolmogorow spectral density (solid line) and power law approximation in the inertial range (dotted line).

to define a fractional Brownian motion or an ARFIMA time series. The new model is then carefully validated using data on turbulent water velocities in the Great Lakes region. It is demonstrated that the model effectively captures both the correlation properties and the underlying probability distribution of these data. Hence it provides the ability to simulate realistic turbulence time series of any length.

2. Tempered fractional calculus

Fractional derivatives were invented by Leibnitz, soon after their more familiar integer-order analogues, but did not become popular in applications until the last few decades. They are now important in virtually every area of science and engineering. The simplest description of a fractional derivative uses the Fourier transform. If $f(x)$ is a function with Fourier transform $F(k) = \int e^{-ikx} f(x) dx$, then the (Riemann–Liouville) fractional derivative $D^\alpha f(x)$ is the function with Fourier transform $(ik)^\alpha F(k)$, extending the familiar integer-order formula [10–12]. Recently, researchers have begun exploring the tempered fractional derivative $D^{\alpha,\lambda} f(x)$, defined as the function with Fourier transform $(\lambda + ik)^\alpha F(k)$, along with its inverse, the tempered fractional integral $I^{\alpha,\lambda} f(x)$, whose Fourier transform is $(\lambda + ik)^{-\alpha} F(k)$ [13–16]. Because of tempering, the Fourier symbol $(\lambda + ik)^{-\alpha}$ does not blow up at the origin, making the tempered fractional calculus simpler and more well-behaved from an abstract mathematical point of view.

Remark. The tempered fractional derivative has also been applied in poroelasticity, where it is called the 'shifted fractional derivative' [17]. It should not be confused with the material derivative (substantial derivative) [18–20] where λ represents the Laplace transform variable, corresponding to a first derivative in time.

3

Tempered fractional derivatives are the limits of tempered fractional difference quotients. We define the tempered fractional difference operator

$$\Delta_h^{\alpha,\lambda} f(x) = \sum_{j=0}^{\infty} w_j \mathrm{e}^{-\lambda jh} f(x - jh) \quad \text{with} \quad w_j := (-1)^j \begin{pmatrix} \alpha \\ j \end{pmatrix} = \frac{(-1)^j \Gamma(1+\alpha)}{j! \Gamma(1+\alpha-j)} \tag{1}$$

for $\alpha > 0$ and $\lambda > 0$, where $\Gamma(\cdot)$ is the Euler gamma function. Then we have

$$D^{\alpha,\lambda} f(x) = \lim_{h \to 0} h^{-\alpha} \Delta_h^{\alpha,\lambda} f(x)$$

whenever f and its derivatives up to order $n > 1+\alpha$ exist and are absolutely integrable [21, Theorem 5.1]. If $\lambda = 0$ and α is a positive integer, then equation (1) reduces to the usual definition of the derivative as the limit of a difference quotient.

The fractional difference operator (1) can also be useful in time series analysis. The ARMA(p, q) model, which combines an autoregression of order p with a moving average of order q, is defined by

$$X_t - \sum_{j=1}^{p} \phi_j X_{t-j} = Z_t + \sum_{i=1}^{q} \theta_i Z_{t-i} \tag{2}$$

where $\{Z_t\}$ is an i.i.d. sequence of uncorrelated random variables (white noise). We say that X_t follows an ARTFIMA(p, α, λ, q) model if

$$Y_t := \Delta_1^{\alpha,\lambda} X_t = \sum_{j=0}^{\infty} w_j \mathrm{e}^{-\lambda j} X_{t-j}$$

follows an ARMA(p, q) model. Then we also have $X_t = \Delta_1^{-\alpha,\lambda} Y_t$, a tempered fractionally integrated ARMA(p, q) model. The fractional integration operator $\Delta_1^{-\alpha,\lambda}$, the inverse of $\Delta_1^{\alpha,\lambda}$, is also defined by (1).

The spectral density

$$f_X(k) = \sum_{j=-\infty}^{+\infty} \mathrm{e}^{ikh} \gamma(h)$$

of a stationary time series X_t with mean zero is the discrete Fourier transform of its covariance function $\gamma(h) = \mathbb{E}[X_t X_{t+h}]$. For a white noise sequence Z_t of i.i.d. random variables with mean $\mathbb{E}[Z_t] = 0$ and variance $\mathbb{E}[Z_t^2] = \sigma^2$, the spectral density $f_Z(k) = \sigma^2/(2\pi)$ is a constant. Using the backward shift operator $BX_t = X_{t-1}$, one can write the time series $X_t = \sum_j \psi_j Z_{t-j}$ in the form $X_t = \Psi(B) Z_t$ where $\Psi(z) = \sum_j \psi_j z^j$. Then the general theory of linear filters implies that X_t has spectral density $f_X(k) = |\Psi(\mathrm{e}^{-ik})|^2 f_Z(k)$ using the complex absolute value (e.g. see [22]). For example, the ARMA(p, q) model $\Phi(B) X_t = \Theta(B) Z_t$ with $\Phi(z) = 1 - \phi_1 z - \cdots - \phi_p z^p$ and $\Theta(z) = 1 + \theta_1 z + \cdots \theta_q z^q$ can be written in the form $X_t = \Psi(B) Z_t$, where $\Psi(z) = \Theta(z)/\Phi(z)$, and hence its spectral density is

$$f_X(k) = \frac{|\Theta(\mathrm{e}^{-ik})|^2}{|\Phi(\mathrm{e}^{-ik})|^2} f_Z(k).$$

Since the tempered fractional difference operator

$$\Delta_1^{\alpha,\lambda} = \sum_{j=0}^{\infty} (-1)^j \begin{pmatrix} \alpha \\ j \end{pmatrix} \mathrm{e}^{-\lambda j} B^j = (1 - \mathrm{e}^{-\lambda} B)^{\alpha}$$

in operator notation, a similar argument shows that the spectral density of an ARTFIMA(p, α, λ, q) time series is given by

$$f_X(k) = \sigma^2 \frac{|\Theta(\mathrm{e}^{-\mathrm{i}k})|^2}{|\Phi(\mathrm{e}^{-\mathrm{i}k})|^2} \left| 1 - \mathrm{e}^{-(\lambda+\mathrm{i}k)} \right|^{-2\alpha}. \tag{3}$$

Remark 2.1. Peiris [23] has proposed a generalized autoregressive GAR(p) time series model $(1 - \beta B)^\alpha X_t = Z_t$ for applications in finance, where $|\beta| < 1$. Taking $\beta = \mathrm{e}^{-\lambda}$ we obtain the ARTFIMA($0, \alpha, \lambda, 0$) model. $\qquad\square$

Kolmogorov [1] argued that the spectral density of turbulent velocity data in the inertial range should be proportional to $k^{-5/3}$ for moderate frequencies k. The simplest time series model with this property is the ARFIMA($0, \alpha, 0$). Its spectral density, obtained by taking $\lambda = 0$ in equation (3), is proportional to $|1-\mathrm{e}^{-\mathrm{i}k}|^{-2\alpha} \sim |k|^{-2\alpha}$ as $|k| \to 0$. Taking $\alpha = 5/6$, we obtain a time series model for turbulence that follows the Kolmogorov spectrum in the inertial range. The more general ARTFIMA($0, \alpha, \lambda, 0$) model has spectral density proportional to $\left| \mathrm{e}^{-(\lambda+k)} - 1 \right|^{-2\alpha} \approx (\lambda^2 + k^2)^{-\alpha}$ when k, λ are sufficiently small. For small values of the tempering parameter λ, the spectral density of an ARTFIMA($0, \alpha, \lambda, 0$) time series grows like $k^{-2\alpha}$ as $|k|$ decreases, but remains bounded as $|k| \to 0$, in agreement with the general theory of turbulence illustrated in figure 1. In the next section, we will fit both the ARFIMA($0, \alpha, 0$) and ARTFIMA($0, \alpha, \lambda, 0$) to turbulent velocity data, to demonstrate the the more general ARTFIMA model is capable of capturing the spectrum of turbulence over the entire range of frequencies.

3. Applications

We used geophysical flow datasets in our analysis including water velocity data from Lakes Michigan and Huron and the Red Cedar River in Michigan. The Lake Huron water data were collected during years 2009–2010 using a 300 kHz RD Instruments acoustic Doppler current profiler (ADCP) at the mouth of the Saginaw Bay (GPS coordinates: 44.2699 N, 83.2609 W) where the depth is approximately 27 m [24]. Data used for analysis in this paper are taken from a vertical bin located approximately 9 m above the lake bottom. Velocity data associated with turbulent supercritical flow in the Red Cedar River, a fourth-order stream in Michigan (Coordinates: 42.72908 N, 84.48228 W) were collected at a sampling rate of 50 Hz using a 16 MHz Sontek Micro-ADV (Acoustic Doppler Velocimeter) on May 26, 2014. Hydrodynamic data were collected in southern Lake Michigan (coordinates: 41.71059 N, 87.20996 W) during summer 2008 using a 600 kHz RDI Workhorse Monitor ADCP in 18.3 m depth using 1 m vertical bins and a sampling rate of 1 Hz as described in [25]. Data from bins 9 and 6 are used here for spectral analysis. Turbulent flow fields have been variously hypothesized as consisting of superimposed waves, or coherent localized vortices or superimposed wave packets with intermittence or pure noise. These datasets contain flow features over a range of spatial and temporal scales associated with turbulent flows in the natural environment and are believed to be appropriate for analysis of energy spectra.

We first consider the dataset for Saginaw Bay, Lake Huron, Michigan, USA (station SB32 in [24]). Complex, unsteady turbulent flow patterns have been noted near the station where data were collected [26]. The log-log plot of the spectrum (periodogram) for these
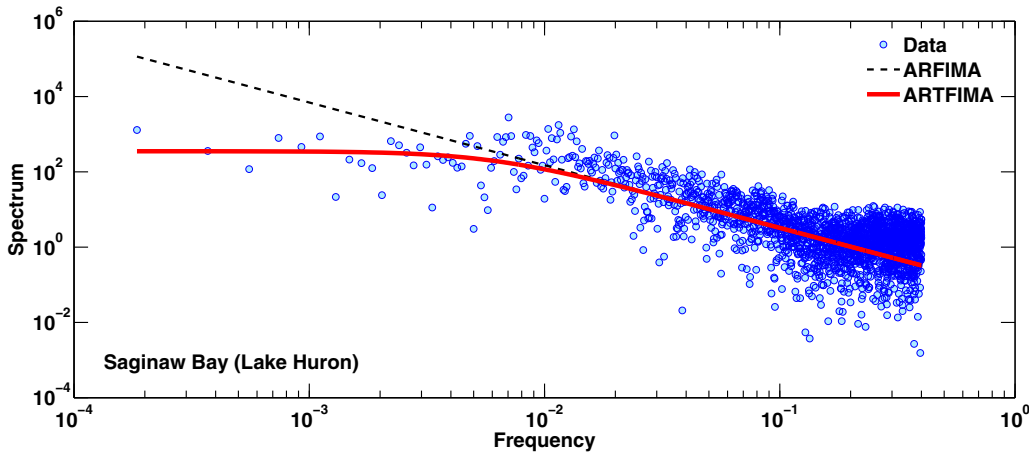
Figure 2. Spectral density of water velocity data, along with fitted ARTFIMA spectrum (thick line), and Kolmogorov spectrum with slope $-5/3$ (thin dashed line). Since the data falls below the straight line at low frequencies, the ARTFIMA model provides a better fit.

data in figure 2 shows a typical linear pattern, indicating a power law spectrum. In this and other geophysical datasets whose spectra have been reported in the literature, the behavior of the spectrum for low values of the frequency k is controlled by several factors including the large-scale current patters and their evolution. Unlike laboratory-scale flows, turbulence in geophysical flows evolves in the presence of a current that varies over much larger scales than the energy-containing scales of turbulence. In addition, shear, stratification and the proximity of boundaries are all known to influence the production of turbulence and hence influence the behavior of the spectrum at low k values.

Consistent with the Kolmogorov theory of turbulence in the inertial range, we find a good fit to a straight line (the thin dashed line in figure 2) with slope $-5/3$ for moderate frequencies, i.e. the spectrum is proportional to $k^{-5/3}$ where k is the frequency. The thick line in figure 2 is the spectrum (3) of the best fitting ARTFIMA$(0, \alpha, \lambda, 0)$, with $\alpha = 5/6$ and tempering parameter $\lambda = 0.006$. Since the data spectrum falls off from the straight line on a log-log plot for low frequencies, the ARTFIMA spectral density provides a better fit. In fact, the apparently straight line plotted in figure 2 is actually the power spectrum (3) of the simpler ARTFIMA$(0, \alpha, \lambda, 0)$ process with $\alpha = 5/6$ and $\lambda = 0$. The deviation from a straight line is impossible to detect at these frequencies. Hence, while the simpler ARFIMA model provides a reasonable approximation in the inertial range, the ARTFIMA model based on tempered fractional calculus provides a suitable time series model for turbulence in the inertial range, and also successfully captures the spectrum in the low frequency (eddy production) range.

To further delineate the ARTFIMA model for this data, we examine the model residuals. First we apply a tempered fractional difference with $\lambda = 0.006$ and $\alpha = 5/6$ to the Saginaw Bay velocity data X_t. Then we compute the autocorrelations of the filtered data $Z_t = \Delta_1^{\alpha,\lambda} X_t$, to verify that the correlation has been removed. The computed autocorrelations are -0.19, 0.03, 0.10, and 0.02 at lags 1 through 4, and the remaining autocorrelation values are all less than 0.05, indicating that the serial correlations has been successfully removed. Since the differenced data $Z_t = \Delta_1^{\alpha,\lambda} X_t$ is uncorrelated, it
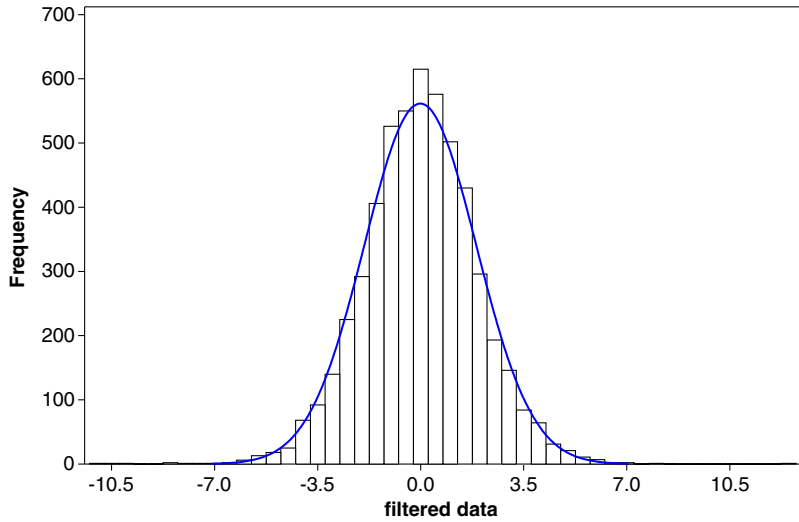
Figure 3. Filtered water velocity data, after applying a tempered fractional difference with $\alpha = 5/6$ and $\lambda = 0.01$, showing a good fit to a normal distribution.
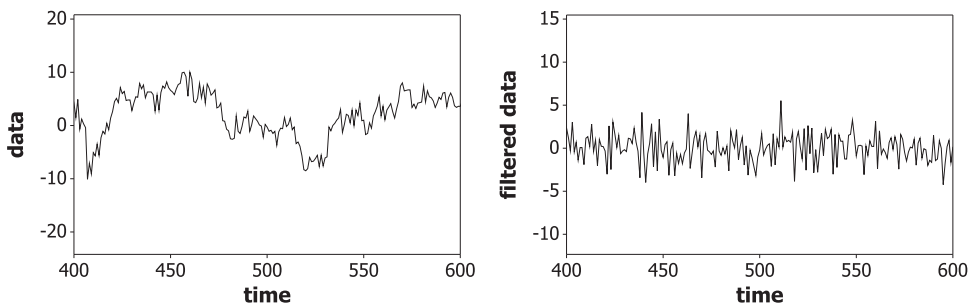

Figure 4. Portion of the water velocity time series (left) and the same data after applying a tempered fractional difference filter with $\alpha = 5/6$ and $\lambda = 0.01$ (right).

follows that the original data $X_t = \Delta_1^{-\alpha,\lambda} Z_t$ fits the ARTFIMA$(0, \alpha, \lambda, 0)$ time series model. Next we examine the distribution of the filtered data Z_t. A histogram of the filtered data is shown in figure 3. The best fitting normal distribution is also shown. Since the data shows a very good fit to the normal density curve with sample mean $-0.02 \approx 0$ and sample standard deviation $\sigma = 1.90$, it follows that the Saginaw Bay velocity data can be accurately modeled as an ARTFIMA$(0, \alpha, \lambda, 0)$, with $\alpha = 5/6$, $\lambda = 0.006$, with $Z_t \sim \mathcal{N}(0, \sigma^2)$.

The left panel in figure 4 shows a portion of the Saginaw Bay velocity data time series. The overall pattern shows long excursions in the same direction (up or down), typical of a stationary increment time series with strong serial autocorrelations. The right panel in figure 4 shows a portion of the same data, after applying a tempered fractional difference filter with $\alpha = 5/6$ and $\lambda = 0.006$. The filtered data (residuals) resemble a Gaussian white noise (uncorrelated) time series, consistent with the ARTFIMA model.

A number of additional data sets were analyzed using the ARTFIMA model. Figure 5 shows three examples. The top panel shows data from Lake Michigan, bin 6, and the
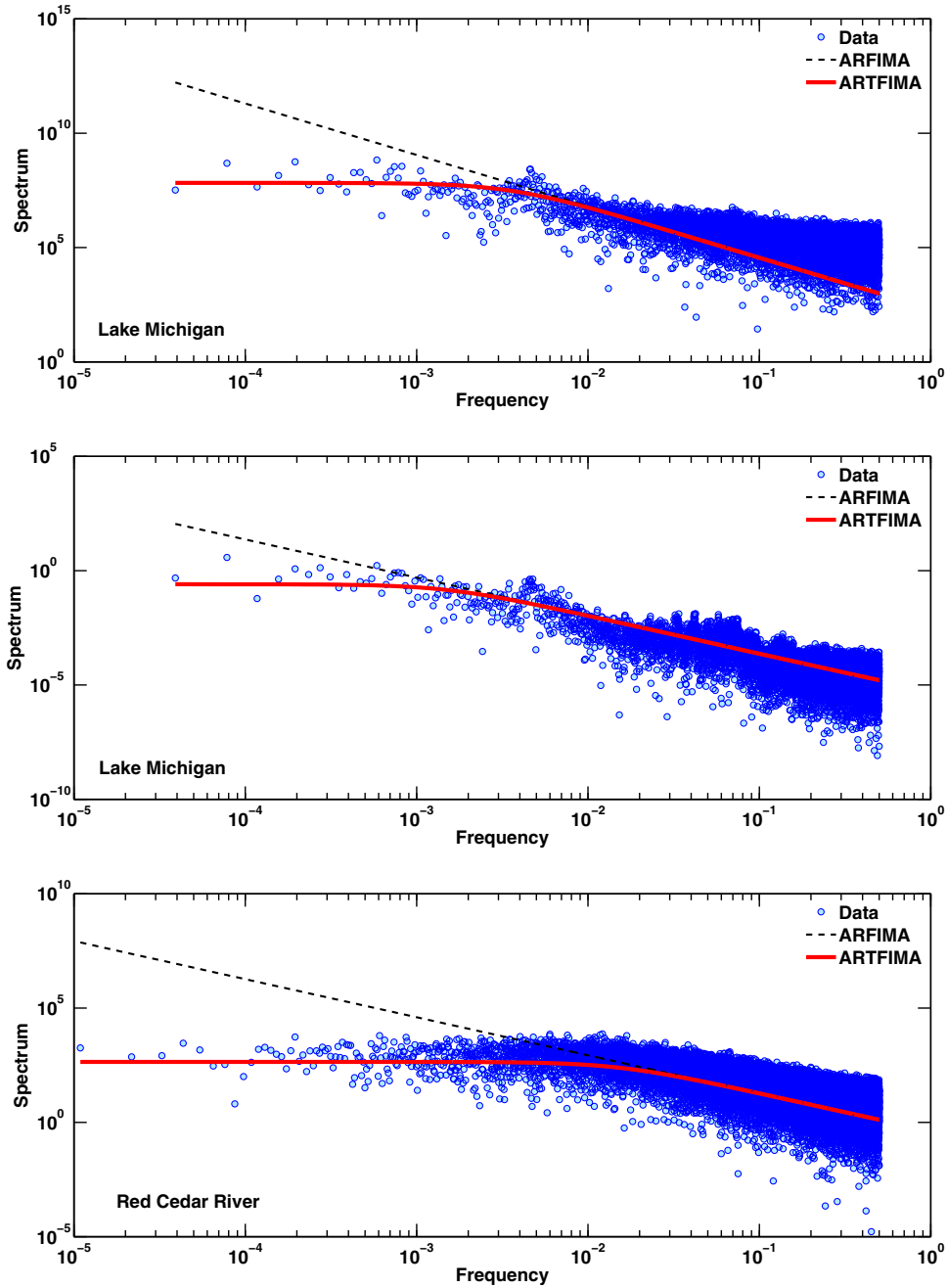
Figure 5. Three additional examples, along with fitted ARTFIMA spectrum (thick line), and Kolmogorov spectrum with slope $-5/3$ (thin dashed line). The data were collected in Lake Michigan (bin 6, top panel; bin 9, middle panel) and the Red Cedar River (bottom panel).

ARTFIMA spectrum with $\alpha = 5/6$ and $\lambda = 0.004$. The middle panel shows data from Lake Michigan, bin 9, and the ARTFIMA spectrum with $\alpha = 5/6$ and $\lambda = 0.0015$. The bottom panel shows data from the Red Cedar River, and the ARTFIMA spectrum with $\alpha = 5/6$ and $\lambda = 0.015$. In every case, the ARTFIMA model provides a significantly better fit than the power law (straight line on these log-log plots) Kolmogorov spectral model.

4. Yaglom noise

Yaglom noise [27–29] is a stochastic model for turbulence in continuous time. In this section, we show how the ARTFIMA$(0, \alpha, \lambda, 0)$ time series model can be viewed as a discrete time version of Yaglom noise. Yaglom noise $Y(t)$ is the tempered fractional integral of a white noise. The tempered fractional integral introduced in section 2 can be defined in real space by a convolution [15, definition 2.1]

$$I^{\alpha,\lambda} f(x) = \frac{1}{\Gamma(\alpha)} \int_{-\infty}^{x} f(u)(x-u)^{\alpha-1} \mathrm{e}^{-\lambda(x-u)} \mathrm{d}u, \tag{4}$$

and then a simple calculation, using the formula for the gamma function, shows that $I^{\alpha,\lambda} f(x)$ has the Fourier transform $(\lambda + \mathrm{i}k)^{-\alpha} F(k)$ [15, Lemma 2.6]. Then we can define

$$Y(t) = I^{\alpha,\lambda} W(t) = \frac{1}{\Gamma(\alpha)} \int_{-\infty}^{t} (t-x)^{\alpha-1} \mathrm{e}^{-\lambda(t-x)} W(x) \mathrm{d}x \tag{5}$$

for any $\alpha > 1/2$ and $\lambda > 0$, where the white noise $W(x) = B'(x)$ is the (weak) derivative of a Brownian motion on $x \in \mathbb{R}$ such that $\mathbb{E}[B(x)^2] = \sigma^2 |x|$, see [15, section 4.2]. The stochastic process $Y(t)$ is stationary and Gaussian with mean zero and finite variance

$$\mathbb{E}[Y(t)^2] = \frac{\sigma^2}{\Gamma(\alpha)^2} \int_{-\infty}^{t} (t-x)^{2\alpha-2} \mathrm{e}^{-2\lambda(t-x)} \, \mathrm{d}x = \frac{\sigma^2 \Gamma(2\alpha-1)}{\Gamma(\alpha)^2 (2\lambda)^{2\alpha-1}}.$$

Next, we show that the ARTFIMA$(0, \alpha, \lambda, 0)$ process $X_t = \Delta_1^{-\alpha,\lambda} Z_t$ converges to a Yaglom noise.

Theorem 4.1. *Let $\alpha > 1/2$ and $\lambda > 0$, and suppose that $\{Z_t\}$ is an iid sequence of Gaussian random variables with mean zero and variance $\sigma^2 < \infty$. Then*

$$n^{\frac{1}{2}-\alpha} \Delta_1^{-\alpha,\frac{\lambda}{n}} Z_t \Rightarrow Y(t)$$

in distribution as $n \to \infty$, where $Y(t)$ is the Yaglom noise (5) with $\mathbb{E}[B(x)^2] = \sigma^2 |x|$.

The proof requires a few simple lemmas.

Lemma 4.2. *Given $\alpha > 1/2$ and $\lambda > 0$, define*

$$C_j^{\lambda} = \frac{1}{\Gamma(\alpha)} j^{\alpha-1} \mathrm{e}^{-\lambda j} \quad \text{for } j \geqslant 1, \text{and} \quad C_j^{\lambda} = 0 \quad \text{otherwise.} \tag{6}$$

Then as $n \to \infty$ as have

$$n^{1-2\alpha} \sum_{j=0}^{\infty} \left| C_j^{\frac{\lambda}{n}} \right|^2 \to \frac{1}{\Gamma(\alpha)^2} \int_{-\infty}^{t} \left| (t-x)^{\alpha-1} \mathrm{e}^{-\lambda(t-x)} \right|^2 \, \mathrm{d}x. \tag{7}$$

Proof. For any t real, a change of variable $j = [nt] - m$ in the sum yields

$$n^{1-2\alpha} \sum_{j=0}^{\infty} \left| C_j^{\frac{\lambda}{n}} \right|^2 = n^{1-2\alpha} \sum_{j=0}^{\infty} \left| \frac{1}{\Gamma(\alpha)} j^{\alpha-1} \mathrm{e}^{-\frac{\lambda}{n} j} \right|^2$$

$$= \frac{n^{1-2\alpha}}{\Gamma(\alpha)^2} \sum_{m=-\infty}^{[nt]} \left| ([nt] - m)^{\alpha-1} \mathrm{e}^{-\frac{\lambda}{n}([nt]-m)} \right|^2$$

$$= \frac{1}{\Gamma(\alpha)^2} \left\{ \frac{1}{n} \sum_{m=-\infty}^{[nt]} \left| \left(\frac{[nt]}{n} - \frac{m}{n} \right)^{\alpha-1} \exp\left[-\lambda \left(\frac{[nt]}{n} - \frac{m}{n} \right) \right] \right|^2 \right\}$$

$$\to \frac{1}{\Gamma(\alpha)^2} \int_{-\infty}^{t} \left| (t-x)^{\alpha-1} e^{-\lambda(t-x)} \right|^2 \, dx$$

as $n \to \infty$ by the definition of the Riemann integral. $\qquad\square$

Lemma 4.3. *Given $\alpha > 1/2$ and $\lambda > 0$, define*

$$\omega_j^\lambda = (-1)^j \binom{-\alpha}{j} e^{-\lambda j} \quad \text{for } j \geqslant 0. \tag{8}$$

Then as $n \to \infty$ as have

$$n^{1-2\alpha} \sum_{j=0}^{\infty} \left| \omega_j^{\frac{\lambda}{n}} \right|^2 \to \frac{1}{\Gamma(\alpha)^2} \int_{-\infty}^{t} \left| (t-x)^{\alpha-1} e^{-\lambda(t-x)} \right|^2 \, dx. \tag{9}$$

Proof. It follows from Stirling's approximation that

$$\omega_j^{\frac{\lambda}{n}} = (-1)^j \binom{-\alpha}{j} e^{-\frac{\lambda}{n}} \sim \frac{\alpha}{\Gamma(1+\alpha)} j^{\alpha-1} e^{-\frac{\lambda}{n}} = C_j^{\frac{\lambda}{n}} \quad \text{as } j \to \infty,$$

where C_j^λ is from (6), see [11, p 24]. Hence for any $\epsilon > 0$ there exists some positive integer N such that

$$(1-\epsilon)C_j^{\frac{\lambda}{n}} < \omega_j^{\frac{\lambda}{n}} < (1+\epsilon)C_j^{\frac{\lambda}{n}} \tag{10}$$

for all $j > N$.

It follows that

$$\lim_{n\to\infty} n^{1-2\alpha} \sum_{j=0}^{\infty} |\omega_j^{\frac{\lambda}{n}}|^2 \leqslant \lim_{n\to\infty} n^{1-2\alpha} \Big[\sum_{j=0}^{N} |\omega_j^{\frac{\lambda}{n}}|^2 + (1+\epsilon)^2 \sum_{j=N+1}^{\infty} |C_j^{\frac{\lambda}{n}}|^2 \Big] \tag{11}$$

$$\leqslant \lim_{n\to\infty} n^{1-2\alpha} \Big[\sum_{j=0}^{N} |\omega_j^{\frac{\lambda}{n}}|^2 + (1+\epsilon)^2 \sum_{j=0}^{\infty} |C_j^{\frac{\lambda}{n}}|^2 \Big]$$

$$\leqslant \frac{(1+\epsilon)^2}{\Gamma(\alpha)^2} \int_{-\infty}^{t} \left| (t-x)^{\alpha-1} e^{-\lambda(t-x)} \right|^2 \, dx,$$

since $\lim_{n\to\infty} n^{1-2\alpha} \sum_{j=0}^{N} |\omega_j^{\frac{\lambda}{n}}|^2 = 0$. Similarly, $n^{1-2\alpha} \sum_{j=0}^{N} |C_j^{\frac{\lambda}{n}}|^2 \to 0$, so that

$$\lim_{n\to\infty} n^{1-2\alpha} \sum_{j=0}^{\infty} |\omega_j^{\frac{\lambda}{n}}|^2 \geqslant \lim_{n\to\infty} n^{1-2\alpha} \Big[\sum_{j=0}^{N} |\omega_j^{\frac{\lambda}{n}}|^2 + (1-\epsilon)^2 \sum_{j=N+1}^{\infty} |C_j^{\frac{\lambda}{n}}|^2 \Big]$$

$$= (1-\epsilon)^2 \lim_{n\to\infty} n^{1-2\alpha} \sum_{j=0}^{\infty} |C_j^{\frac{\lambda}{n}}|^2$$

$$= \frac{(1-\epsilon)^2}{\Gamma(\alpha)^2} \int_{-\infty}^{t} \left| (t-x)^{\alpha-1} e^{-\lambda(t-x)} \right|^2 \, dx$$

by lemma 4.2. Since $\epsilon > 0$ is arbitrary, (9) follows. $\qquad\square$

Proof of theorem 4.1. Compute the characteristic function of $n^{\frac{1}{2}-\alpha}\Delta_1^{-\alpha,\frac{\lambda}{n}}Z_t$ and take the limit as $n \to \infty$ using lemma 4.3 to see that

$$\lim_{n\to\infty} \mathbb{E}\Big[\exp\{\mathrm{i}\theta n^{\frac{1}{2}-\alpha}\Delta_1^{-\alpha,\frac{\lambda}{n}}Z_t\}\Big] = \exp\left\{-\lim_{n\to\infty} n^{1-2\alpha}\theta^2\sigma^2 \sum_{j=0}^{\infty}\Big|\omega_j^{\frac{\lambda}{n}}\Big|^2\right\}$$

$$= \exp\left\{-\frac{\theta^2\sigma^2}{\Gamma(\alpha)^2}\int_{-\infty}^{t}\Big|(t-x)^{\alpha-1}\mathrm{e}^{-\lambda(t-x)}\Big|^2\,\mathrm{d}x\right\}$$

$$= \mathbb{E}\left[\exp\{\mathrm{i}\theta Y(t)\}\right].$$

Since convergence of characteristic functions implies convergence in distribution, this completes the proof. □

Theorem 4.1 shows that the ARTFIMA$(0,\alpha,\lambda,0)$ time series is a discrete time version of a Yaglom noise. Next we recall some properties of Yaglom noise, and compare to the ARTFIMA model. To make the paper self-contained, we include some details, see also [30]. The stochastic integral $I(f) = \int f(x)W(x)\mathrm{d}x$ defines a Gaussian random variable such that $I(f)I(g) = \sigma^2 \int f(x)g(x)\mathrm{d}x$ for any $f, g \in L^2(\mathbb{R})$ [31, chapter 3]. Hence Yaglom noise has the covariance function

$$\gamma(h) = \mathbb{E}\left[Y(t)Y(t+h)\right]$$

$$= \frac{\sigma^2}{\Gamma(\alpha)^2}\int_{-\infty}^{t} \mathrm{e}^{-\lambda(t-x)}(t-x)^{\alpha-1}\mathrm{e}^{-\lambda(t+h-x)}(t+h-x)^{\alpha-1}\,\mathrm{d}x$$

$$= \frac{\sigma^2}{\Gamma(\alpha)^2}\int_{0}^{\infty} \mathrm{e}^{-\lambda(y+h)}(y+h)^{\alpha-1}\mathrm{e}^{-\lambda y}y^{\alpha-1}\,\mathrm{d}y$$

$$= \frac{\sigma^2}{\Gamma(\alpha)^2}\int_{0}^{\infty} \mathrm{e}^{-2\lambda y}\mathrm{e}^{-\lambda(h)}(y+h)^{\alpha-1}y^{\alpha-1}\,\mathrm{d}y$$

$$= \frac{\sigma^2}{\Gamma(\alpha)\sqrt{\pi}}\Big(\frac{h}{2\lambda}\Big)^{\alpha-\frac{1}{2}}K_{\frac{1}{2}-\alpha}(\lambda h).$$

using integral formula No. 8 on p. 344 of Gradshteyn and Ryzhik [32]. The spectral density of Yaglom noise is the inverse Fourier transform of its covariance function:

$$f_Y(k) = \frac{1}{2\pi}\int_{-\infty}^{\infty} \mathrm{e}^{\mathrm{i}kx}\gamma(x)\,\mathrm{d}x$$

$$= \frac{\sigma^2}{\Gamma(\alpha)\sqrt{\pi}(2\lambda)^{\alpha-\frac{1}{2}}}\int_{-\infty}^{\infty}\cos(kx)|x|^{\alpha-\frac{1}{2}}K_{\frac{1}{2}-\alpha}(\lambda|x|)\,\mathrm{d}x$$

$$= \frac{\sigma^2}{\Gamma(\alpha)\sqrt{\pi}(2\lambda)^{\alpha-\frac{1}{2}}}\sqrt{\pi}(2\lambda)^{\alpha-\frac{1}{2}}\Gamma(\alpha)(\lambda^2+k^2)^{-\alpha}$$

$$= \sigma^2(\lambda^2+k^2)^{-\alpha},$$

using formula [32, No 12, p 724] to evaluate the integral in the second line. As noted at the end of section 2, the spectrum of an ARTFIMA$(0,\alpha,\lambda,0)$ time series is proportional to $\left|\mathrm{e}^{-(\lambda+\mathrm{i}k)}-1\right|^{-2\alpha} \approx (\lambda^2+k^2)^{-\alpha}$ when k, λ are sufficiently small, connecting the spectral behavior of the ARTFIMA model to Yaglom noise. Both follow the Kolmogorov model $f(k) \approx k^{-5/3}$ for turbulence when $\alpha = 5/6$.

4.1. Tempered fractional Gaussian noise

Tempered fractional Gaussian noise (TFGN) is a stationary time series which can be defined by $X_t := Y(t) - Y(t-1)$, where $Y(t)$ is the Yaglom noise (5). Then it follows immediately from the theory of linear filters that its spectral density is given by

$$f(k) = \frac{\sigma^2}{2\pi} \left| e^{-ik} - 1 \right|^2 (\lambda^2 + k^2)^{-\alpha} \qquad (12)$$

for all real k, see also [33, section 4]. A Taylor expansion shows that $\left| e^{-ik} - 1 \right|^2 = 2 - 2\cos k \sim k^2$ as $k \to 0$. If the tempering parameter λ is sufficiently small, then the spectral density grows like the divergent power law $k^{2-2\alpha}$ as k decreases, and we can take $\alpha = 11/6$ to recover the Kolmogorov spectrum. Hence TFGN can provide another alternative time series model for turbulence. However, the ARTFIMA model has the advantage that the tempered fractional difference filter can be easily inverted, as we did for figure 3, to obtain the model residuals. Furthermore, the TFGN spectrum tends to zero as $k \to 0$, whereas the ARTFIMA spectrum levels off. For applications to geophysics, the ARTFIMA spectrum seems to provide a more suitable model, see figures 2 and 5.

References

[1] Kolmogorov A N 1940 *Dokl. Akad. Nauk SSSR* **26** 115
[2] Friedlander S K and Topper L (ed) 1961 *Turbulence: Classical Papers On Statistical Theory* (New York: Interscience)
[3] Shiryaev A N 1999 *Kolmogorov and the Turbulence* (University of Aarhus: Centre for Mathematical Physics and Stochastics)
[4] Mandelbrot B and Van Ness J 1968 *SIAM Rev.* **10** 422
[5] Grant H, Moilliet L A and Vogel W M 1968 *J. Fluid Mech.* **34** 443
[6] Dillon T M and Powell T M J 1976 *Geophys. Res.* **81** 6421
[7] Kaimal J C, Wyngaard J C, Izumi Y and Cote O R 1972 *Q. J. R. Meteorol. Soc.* **98** 563
[8] Pérez Beaupuits J P, Otárola A, Rantakyrö FT, Rivera R C, Radford S J E and Nyman L-Å 2004 Analysis of wind data gathered at Chajnantor *ALMA Memo* **497**
[9] Tennekes H and Lumley J L 1972 *A First Course in Turbulence* (Cambridge, MA: MIT Press)
[10] Mainardi F 2010 *Fractional Calculus and Waves in Linear Viscoelasticity: an Introduction to Mathematical Models* (Hackensack, NJ: Imperial College Press)
[11] Meerschaert M M and Sikorskii A 2012 *Stochastic Models for Fractional Calculus* (Berlin: De Gruyter)
[12] Samko S G, Kilbas A A and Marichev O I 1993 *Fractional Integrals and Derivatives* (London: Gordon and Breach)
[13] Baeumer B and Meerschaert M M 2010 *J. Comput. Appl. Math.* **233** 2438
[14] Cartea Á and del-Castillo-Negrete D 2007 *Phys. Rev.* E **76** 041105
[15] Meerschaert M M and Sabzikar F 2014 *Stochastic Process. Appl.* **124** 2363
[16] Meerschaert M M, Zhang Y and Baeumer B 2008 *Geophys. Res. Lett.* **35** 17403
[17] Hanyga A, 2001 *Math. Computer Modelling* **34** 1399
[18] Friedrich R, Jenko F, Baule A and Eule S 2006 *Phys. Rev. Lett.* **96** 230601
[19] Turgeman L, Carmi S and Barkai E 2009 *Phys. Rev. Lett.* **103** 190201
[20] Sokolov I M and Metzler R 2003 *Phys. Rev.* E **67** 010101(R)
[21] Sabzikar F, Meerschaert M M and Chen J 2014 Tempered fractional calculus *J. Comput. Phys.* to appear doi: 10.1016/j.jcp.2014.04.024
[22] Brockwell P J and Davis R A 1991 *Time Series: Theory and Methods* 2nd edn (New York: Springer)
[23] Peiris M S 2003 *Stat. Methods* **5** 172
[24] Nguyen T D 2014 *PhD Dissertation* Department of Civil and Environmental Engineering, Michigan State University, East Lansing
[25] Thupaki P, Phanikumar M S and Whitman R L 2013 *J. Geophys. Res. Oceans* **118** 1606

[26] Nguyen T D, Thupaki P and Anderson E J and Phanikumar M S 2014 *J. Geophys. Res. Oceans* **119** 2713
[27] Monin A S and Yaglom A M 1975 *Statistical Fluid Mechanics* vol 2 (Cambridge, MA: MIT press)
[28] Yaglom A M 1987 *Correlation Theory of Stationary and Related Random Functions I* (New York: Springer)
[29] Yaglom A M 1987 *Correlation Theory of Stationary and Related Random Functions II* (New York: Springer)
[30] Lim S C and Eab C H 2006 *Phys. Lett.* A **355** 87
[31] Samorodnitsky G and Taqqu M 1994 *Stable Non-Gaussian Random Processes* (New York: Chapman and Hall)
[32] Gradshteyn I S and Ryzhik I M 2000 *Table of Integrals and Products* 6th edn (San Diego: Academic)
[33] Meerschaert M M and Sabzikar F 2013 *Stat. Probab. Lett.* **83** 2269